Controlling Dispersive Chaos in Binary-Fluid Convection

Paul Kolodner,[1] Georg Flätgen,[1,2,3] and Ioannis G. Kevrekidis[3]
[1]*Bell Laboratories, Lucent Technologies, Inc., Murray Hill, New Jersey*
[2]*Fritz-Haber-Institut der Max-Planck-Gesellschaft, Berlin, Germany*
[3]*Department of Chemical Engineering, Princeton University, Princeton, New Jersey*
(Received 11 February 1999)

We report observations of stabilized traveling-wave (TW) convection in a regime in which the uncontrolled system exhibits repeated, erratic growth and abrupt decay of spatially localized bursts of TW. By applying as feedback a spatially varying Rayleigh-number profile computed from the measured convection pattern, we suppress this behavior and stabilize states of unidirectional TW with spatially uniform amplitude on the unstable branch of the subcritical bifurcation to convection. This allows us to measure the nonlinear coefficients of the corresponding quintic complex Ginzburg-Landau equation.

PACS numbers: 47.20.Ky, 05.45.Gg, 47.54.+r, 47.62.+q

The work of Ott, Grebogi, and Yorke awakened interest among physicists in using feedback to control unstable dynamical behavior in systems which are chaotic in the absence of control [1]. It is often possible to maintain such systems in unstable but regular dynamical states by making small changes to a global control parameter in response to deviations of the measured dynamics from the target state [2]. However, extending such feedback techniques to the control of erratic patterns in spatially extended systems remains a difficult and open problem. Computationally, there has been some success in applying spatially varying feedback to control spatiotemporal chaos in coupled-map lattices [3] and in continuum systems [4]. Experimentally, it is sometimes possible to reduce erratic pattern dynamics to a chaotic single-channel signal, which can then be controlled using temporal chaos-control techniques [5]. But full control of erratic patterns in a spatially extended system, using spatially distributed feedback, has yet to be demonstrated.

In this paper, we describe experiments on a spatially extended pattern-forming system in which erratic behavior has been suppressed by using spatially distributed feedback. We study convection in a thin, horizontal layer of an ethanol-water mixture which is heated from below, in a periodic, quasi-one-dimensional geometry. The control parameter is the Rayleigh number R, which is proportional to the temperature different applied vertically across the fluid layer, and we define a stress parameter $\varepsilon \equiv (R - R_c)/R_c$, where R_c is the threshold Rayleigh number for the onset of convection. In this system, the first instability is oscillatory, and it triggers a subcritical bifurcation to a nonlinear state of traveling waves (TWs). For the parameters of the present experiments, the first nonlinear TW state seen above R_c is known as "dispersive chaos" and is characterized by the repeated, erratic appearance and sudden collapse of spatially localized bursts of TW [6]. By applying a spatially varying stress-parameter profile, computed from real-time, spatially resolved measurements of the complex TW amplitude, we have stabilized a state of unidirectional TW with the spatially uniform amplitude and wave number far onto an unstable TW branch which is born from the quiescent state via a subcritical bifurcation. By tracing this unstable branch, we have accurately measured the coefficients of the fifth-order complex Ginzburg-Landau equation (CGLE) which describes the bifurcation. Related techniques have been used to stabilize the quiescent state above the onset of steady convection in a pure fluid [7].

The experimental system has previously been described in detail [8]. The convection cell is a long, narrow annulus, formed by a plastic disk and ring which are clamped between a mirror-polished, silicon bottom plate and a transparent, sapphire top plate. The annular channel has height $d = 0.2597(2)$ cm, radial width $\Gamma_r = 2.074(3)d$, and mean circumference $\Gamma_\phi = 91.10(8)d$. The cell is filled with a 0.4 wt % solution of ethanol in water at mean temperature 27.60 °C, with separation ratio $\psi = -0.020$, Prandtl number $\mathrm{Pr} = 5.92$, and Lewis number $L = 0.0085$ [9]. Wave numbers and frequencies are rendered nondimensional by scaling with the cell height d and the vertical thermal diffusion time $\tau_v = 45.8$ sec, respectively.

The top plate of the convection cell is cooled by temperature-controlled, circulating water, and the bottom plate is electrically heated by two systems. The main heater is a round, thin-film heater glued to the underside of the plate. To apply spatially varying Rayleigh-number profiles, a second heating system is used, consisting of 24 small resistors, pressed against the underside of the bottom plate in a ring just outside the footprint of the convection cell. These trim heaters are connected in parallel with the main heater, and individually computer-controlled shunt resistors are used to adjust the fractional power dissipated in each. An arbitrary Rayleigh-number profile—including one that is nominally uniform—can be applied with a fractional azimuthal variation of $(1-2) \times 10^{-4}$ rms, as measured using the pulse-drift technique [10], and a temporal stability of $(2-5) \times 10^{-5}$ rms over time scales shorter than a day. Drifts over longer periods are removed as described below and previously [6,8].

In this system, convection patterns can in general take the form of superpositions of clockwise- and

 0031-9007/99/83(4)/730(4)$15.00

counterclockwise-propagating TW, of the form $A(x)\sin[k(x)x \pm \omega(x)t]$. In the experiments described here, the amplitude, wave number, and oscillation frequency $A(x)$, $k(x)$, and $\omega(x)$ vary only on spatial scales much longer than $2\pi/k_m$ (the subscript m denotes the spatial average of the measured profile). Near onset, the typical oscillation period $\tau_{\rm osc} = 2\pi/\omega_m$ is 90–100 sec. The TW pattern is monitored using a shadowgraph system and is recorded at 360 azimuthal locations by a circular array of photodiodes that is sampled by two computers. One computer, used only for independent quantitative data acquisition when the dynamics have been verified to be stable, samples the system at a rate $\sim 4/\tau_{\rm osc}$ for many oscillation cycles. Complex demodulation of this signal [11] is used to extract $A(x)$ and $k(x)$ with a precision of $\pm 3\%$ in A and $\pm 0.2\%$ in k. All of the dynamical states studied here consist of unidirectional TW with mean wave number $k_m = 2\pi N_r/\Gamma_\phi = 3.035$, where $N_r = 44$ is the quantized number of wavelengths filling the convection cell. For unidirectional TW, temporal demodulation of the time series at several spatial points yields the oscillation frequency ω_m with a fractional precision of $\sim 1 \times 10^{-4}$. A second computer, dedicated to fast control of the system, samples the camera signals for short periods at regular intervals and uses a simplified demodulation program to extract $A(x)$ and $k(x)$ in a single temporal oscillation cycle. These profiles are used to compute the feedback Rayleigh-number profile applied to the convection cell.

The set point that is varied in these experiments is the spatially averaged TW amplitude, denoted A_s. Control at a chosen value of A_s causes the amplitude and wave number profiles to become spatially uniform, with values $A_m = A_s$ and $k_m = 3.035$, respectively, the TW frequency to settle to a spatially uniform value $\omega_m(A_s)$, and the Rayleigh number to setting to a value $R(A_s)$. From the measured quantities $R(A_s)$ and $\omega_m(A_s)$, we compute $\varepsilon(A_s) = [R(A_s) - R_{\rm ref}]/R_{\rm ref}$ and $\Delta\omega(A_s) = \omega_m(A_s) - \omega_{\rm ref}$, where $R_{\rm ref}$ and $\omega_{\rm ref}$ are drift-corrected measurements [6,8] made at a reference amplitude, $A_{\rm ref} = 0.0024$, that is smaller than the threshold for any spatial instability.

Each experimental run begins with the creation of unidirectional TW of small amplitude by injecting localized disturbances and suppressing TW that propagate in the undesired direction [10]. Linear dispersion turns the remaining TW into a spatially uniform, unidirectional state in about 10 hours. During this evolution, we apply spatially uniform feedback so as to stabilize the TW amplitude at $A_s = A_{\rm ref}$, using the control algorithm described in [11]. This algorithm consists of periodically subtracting from the Rayleigh number a correction equal to the sum of two components, one proportional to the latest measured growth rate $A_m^{-1} dA_m/dt$ and one proportional to the fractional amplitude error $\ln(A_m/A_s)$. This global feedback is applied during all measurements described in this paper. Once the uniform state is stable, we measure the wave number and amplitude profiles, $A_{\rm ref}(x)$ and $k_{\rm ref}(x)$, for correction of small optical distortions in subsequent measurements [8]. We then increase the set point A_s, let the system settle, and make further measurements of $R(A_s)$, $A(x)$, $k(x)$, and $\omega(x)$.

Previously [6], the nonlinear evolution of this uniform state was studied by turning off the global feedback control and increasing R to a constant value just above onset. A transition to dispersive chaos via a characteristic temporal burst and spatial collapse was observed. Under the global control used here, a similar evolution is seen, but it is triggered by a new instability of the spatially uniform state to growing, propagating amplitude modulations which appear when A_s is increased above a threshold $A_1 \sim 0.0029$. Figure 1 shows the growth of this instability. In the first part of this run, made at $A_s = 0.0030$, the initially uniform amplitude profile develops diagonal stripes of increasing contrast, characteristic of the growth of the lowest spatial Fourier mode. When A_s is increased to 0.0035, the modulation growth rate increases. In the last $\sim$15 hours of this run, when the modulations have grown to high amplitude, they become spatially and temporally nonuniform. The subsequent evolution of the system is erratic and exhibits many of the hallmarks of dispersive chaos without feedback.

Figure 2 shows the dependence on A_s of the growth rate γ_1 and the frequency ω_1 of the amplitude modulations produced by this instability. The zero crossing of γ_1 defines the instability threshold $A_1 = 0.00287(4)$. The modulation frequency $\omega_1 = 0.0497(4)$ is independent of

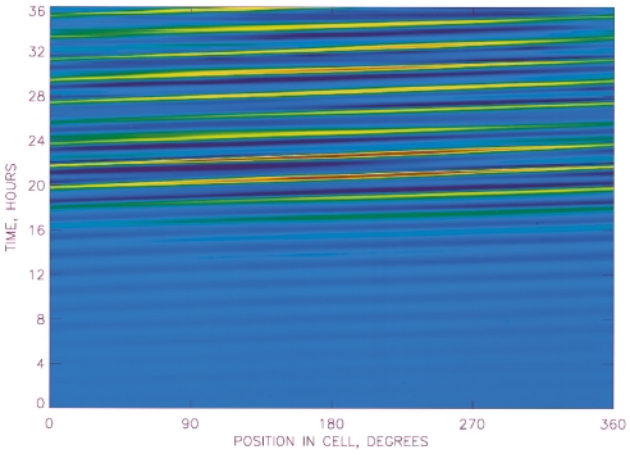

FIG. 1 (color). False-color, space-time representation of the TW amplitude in an initially spatially uniform state of right-going TW, illustrating the growth of propagating amplitude modulations. The color sequence dark blue–light blue–green–yellow–red encodes increasing TW amplitude. Initially, the set point A_s was set to 0.0030, just above the instability threshold A_1, and diagonal stripes of increasing modulation depth reveal the growth of the instability. At time $t = 15$ h, A_s was further increased to 0.0035, accelerating the growth of the modulations and leading to spatial and temporal variations in their strength.

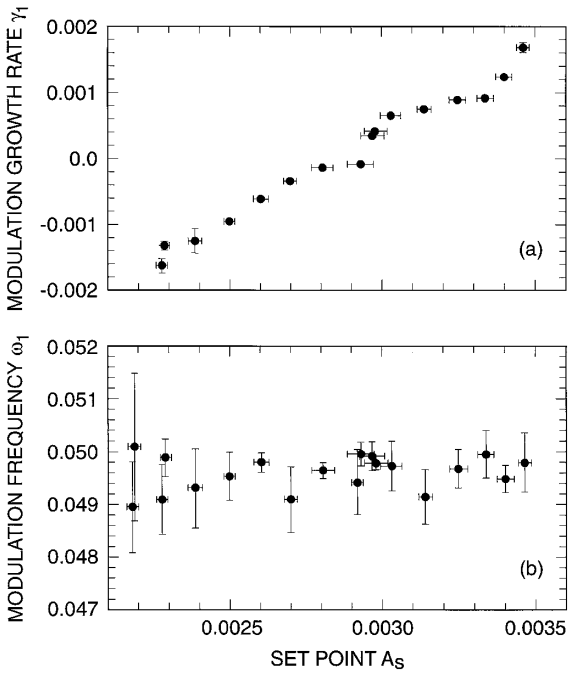

FIG. 2. The dimensionless growth rate (a) and frequency (b) of modulations of the amplitude profile with no spatial feedback are plotted as functions of the set point A_s. Above $A_s = A_1 = 0.00287(4)$, TWs controlled with global feedback alone are unstable and require spatial feedback for stability.

A_s. For comparison, the phase velocity of the underlying TW corresponds to a frequency of 0.072.

We damp these modulations by adding a spatially varying stress-parameter component $\Delta\varepsilon_1(x) = -\chi_1 \ln[A(x + \delta x_d)/A_s]$ to the spatially uniform stress parameter $\varepsilon(A_s)$. Here, $\chi_1 > 0$ is a gain, and $\delta x_d \propto \omega_1$ is a spatial shift set to match the drift of the amplitude modulation during the time delay required to calculate and apply the spatial feedback. For a range of χ_1, turning on this feedback component rapidly eliminates amplitude modulations. As A_s is increased, larger values of χ_1 are required for stabilization.

The TW state controlled by this feedback algorithm is stable up to amplitude $A_2 = 0.01080(2)$. Above this second threshold, propagating wave-number modulations appear. To damp them, we add an additional spatial feedback component $\Delta\varepsilon_2(x) = \chi_2 \partial_x k(x + \delta x_d)$. As before, $\chi_2 > 0$, and a spatial shift compensates for propagation delay. Adding this feedback component to $\varepsilon(A_s) + \Delta\varepsilon_1(x)$ causes wave-number modulations to decay slowly. Again, stabilization at larger amplitudes requires larger gains. The heuristic reason for this choice of feedback algorithm is that, in all nonlinear TW states in binary-fluid convection, the TW phase velocity decreases with increasing Rayleigh number [8]. Thus, since gradients of wave number and of phase velocity are equivalent, they are reduced by feedback proportional to $\partial_x k(x)$.

Above $A_s \sim 0.013$, we observe that the wave number profile in the controlled state develops a static distortion whose magnitude grows with increasing A_s. When $k(x)$ is sufficiently distorted, the coupling between wave number variations and the amplitude growth rate described by Kaplan *et al.* [12] causes the system to become dispersively unstable and impossible to control. This behavior is due to an increasing sensitivity of the wave number profile to small spatial variations in the amplitude profile. These in turn are due to imprecision in the reference profile $A_{\mathrm{ref}}(x)$ measured at low amplitude before the application of spatial feedback. By making small modifications to $A_{\mathrm{ref}}(x)$, using algorithms to be described in a subsequent publication, we can eliminate the wave number distortions that destabilize the system. This allows control of TW up to amplitudes much higher than the second instability threshold A_2. It is important to point out that the sensitivity of $k(x)$ to $A(x)$ is so great that the modifications imposed on $A_{\mathrm{ref}}(x)$ are small—comparable to the precision with which $A(x)$ is computed in the first place. Also, the spatial variation in the Rayleigh-number profile required for stability is only $(2-4) \times 10^{-4}$ for all the data discussed in this paper. Thus, we are indeed stabilizing uniform TW states with spatial feedback of infinitesimal magnitude. We have also verified that the controlled state loses stability when the control is turned off.

Figure 3 shows measurements of $\varepsilon(A_s)$ and $\Delta\omega(A_s)$ for unidirectional TW states controlled with spatial feedback. As shown in Fig. 3(a), the closed feedback loop has allowed us to trace the subcritical open-loop bifurcation diagram up to amplitudes much higher than the thresholds of the two secondary instabilities, which are indicated by horizontal lines. Figure 3(b) shows the amplitude dependence of the oscillation frequency. These data are consistent with the predictions of a quintic, complex Ginzburg-Landau equation (CGLE):

$$\tau_0(\partial_t + s\partial_x)A = \varepsilon(1 + ic_0)A + \xi_0^2(1 + ic_1)\partial_x^2 A + g(1 + ic_2)|A|^2 A + h(1 + ic_4)|A|^4 A\,. \quad (1)$$

Substituting $A(x,t) = A_s e^{i(\Delta\omega t - \Delta k x)}$ into Eq. (1) and dropping terms that are independent of A_s give

$$\varepsilon + gA_s^2 + hA_s^4 = 0\,, \quad (2a)$$

$$\tau_0\Delta\omega = c_2 g A_s^2 + c_4 h A_s^4\,. \quad (2b)$$

Fitting the amplitude dependences shown in Fig. 3 to Eqs. (2a) and (2b) yields $g = 13.2 \pm 0.5$, $\tau_0^{-1}c_2 g = -754 \pm 36$, $h = (-7.1 \pm 1.1) \times 10^3$, and $\tau_0^{-1}c_4 h = (2.1 \pm 1.1) \times 10^5$ [13]. These values have been substituted into Eqs. (2a) and (2b) to produce the solid curves in Figs. 3(a) and 3(b). The cubic coefficients derived from these fits are consistent with the less-precise values obtained from the analysis of onset transients described in Ref. [6]: With $\tau_0^{-1} = 9.81 \pm 0.19$ [6], we obtain a nonlinear frequency-renormalization coefficient

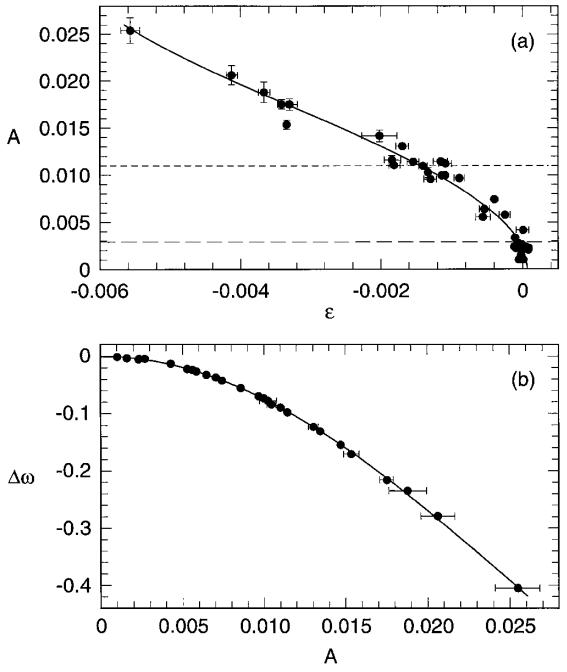

FIG. 3. (a) The stress parameter $\varepsilon(A_s)$ in controlled, uniform TW states is plotted against the set point A_s, with the axes interchanged so as to produce a bifurcation diagram. The subscript s has been dropped to emphasize the point that this is an open-look bifurcation diagram that has been traced in closed loop. The data have been shifted slightly to give $\varepsilon(A_s \to 0) \to 0$. The long- and short-dashed lines show the instability thresholds A_1 and A_2, respectively. These amplitude thresholds correspond to $\varepsilon_1 = -0.00011$ and $\varepsilon_2 = -0.00144$. The curve is a fit to the solution of the CGLE given in Eq. (2a). (b) The oscillation frequency $\Delta\omega(A_s)$ is plotted against A_s. Again, the data are shifted to give $\Delta\omega(A_s \to 0) \to 0$; the actual oscillation frequency at zero amplitude is 3.14. The curve is a fit of the form given in Eq. (2b).

$c_2 = -5.82 \pm 0.37$, consistent with the value -7.5 ± 3.2 reported previously [6]. With $c_1 = 0.0079(33)$ [6], we obtain $1 + c_1 c_2 = 0.954(19)$. The analyses presented in Refs. [6,12] yielded rather imprecise values for the cubic coefficients in the CGLE and are certainly unable to determine the quintic coefficients at all. *The measurement of these coefficients has relied crucially on the ability to stabilize uniform TW using spatial feedback.*

In summary, we have stabilized states of uniform, unidirectional TW in a dispersively unstable regime of binary-fluid convection by applying a spatially varying Rayleigh-number profile computed from measurements of the TW amplitude and wave number profiles. This represents an important demonstration that such feedback can be used to suppress erratic behavior in a spatially extended system. This control has allowed us to make accurate measurements of the nonlinear coefficients of the equation that describes the dynamics of this system.

I. G. K. acknowledges support from the National Science Foundation. G. F. gratefully acknowledges the financial support of the Deutsche Forschungsgemeinschaft.

[1] E. Ott, C. Grebogi, and J. A. Yorke, Phys. Rev. Lett. **64**, 1196 (1990).
[2] T. Shinbrot, Adv. Phys. **44**, 73 (1995).
[3] N. Parekh, S. Parthasarathy, and S. Sinha, Phys. Rev. Lett. **81**, 1401 (1998), and references therein.
[4] M. E. Bleich, D. Hochheiser, J. V. Moloney, and J. E. S. Socolar, Phys. Rev. E **55**, 2119 (1997).
[5] F. Qin, E. E. Wolf, and H.-C. Chang, Phys. Rev. Lett. **72**, 1459 (1994).
[6] P. Kolodner, S. Slimani, N. Aubry, and R. Lima, Physica (Amsterdam) **D85**, 165 (1995).
[7] L. Howle, Int. J. Heat Mass Transf. **40**, 817 (1997); Phys. Fluids **9**, 1861 (1997); J. Tang and H. H. Bau, J. Fluid Mech. **363**, 153 (1998).
[8] P. Kolodner, Phys. Rev. A **46**, 6431 (1992).
[9] P. Kolodner, H. Williams, and C. Moe, J. Chem. Phys. **88**, 6512 (1988).
[10] P. Kolodner, Phys. Rev. A **44**, 6448 (1991); **44**, 6466 (1991).
[11] P. Kolodner and H. Williams, in *Proceedings of the NATO Advanced Research Workshop on Nonlinear Evolution of Spatio-temporal Structures in Dissipative Continuous Systems*, edited by F. H. Busse and L. Kramer, NATO Advanced Study Institutes, Series B2, Vol. 225 (Plenum, New York, 1990), p. 73.
[12] E. Kaplan, E. Kuznetsov, and V. Steinberg, Europhys. Lett. **28**, 237 (1994); Phys. Rev. E **50**, 3712 (1994).
[13] In both cases, dropping the quartic term results in a clearly bad fit. Neither fit is improved significantly if higher-order terms are included.